Proceedings of ASME Turbo Expo 2011
GT2011
June 6-10, 2011, Vancouver, British Columbia, Canada

GT2011-45247

GAS TURBINE NOZZLE LIFE ASSESMENT DUE TO THERMAL FATIGUE

Z. Mazur
Instituto de Investigaciones Eléctricas,
Gerencia de Turbomaquinaria
Av. Reforma No. 113, Col. Palmira
62490 Cuernavaca, Morelos, México

E.B. Pérez-Hernández
GE IQ, Queretaro, México

R. Garcia-Illescas
Instituto de Investigaciones Eléctricas,
Gerencia de Turbomaquinaria
Av. Reforma No. 113, Col. Palmira
62490 Cuernavaca, Morelos, México

ABSTRACT

Available fatigue models are analyzed to assess gas turbine nozzle life due to thermal fatigue cycles experienced in operation. A nozzle retired from service made of cobalt base alloy FSX-414 experienced fatigue cracks during its operation period. Nozzle thermal stresses and strains generated during gas turbine transitions; startups and shut downs, determined in previous investigations are used for fatigue analysis and life assessment. A specialized software nCode was used for fatigue analysis and the Rainflow method to account for fatigue cycles. The fatigue life models of Manson-Coffin-Basquin, Morrow and Smith-Watson-Topper were compared assessing nozzle life in different critical zones of the vane and its union to the internal and external shrouds. Some similarities and deviations found among fatigue models are analyzed. Diagrams of nozzle life distribution within its body are provided. It was found that the nozzle zones having shortest life are located in the vane cooling ducts and transitions/unions between vane and shrouds.

KEYWORDS

Low cycle fatigue; Gas turbine; Nozzle; Vanes; Fatigue models; Useful life assessment.

1 INTRODUCTION

Gas turbines experience thermal transients in most hot components during service. Damage under these thermal loads is a limiting aspect in useful lives especially in blades and nozzles of the first stage. The most recurrent cause of failure in these hot components is thermo-mechanical fatigue whose origin is alternating mechanical and thermal stresses during startups, full load and shutdowns or trips.

In gas turbine components, temperatures and stresses represent the main parameters that directly affect optimum structural performance which, during their lifetime, decrease useful life. These parameters vary depending on time during transients and are related to heat transfer (gas flow and pressure, cooling air flow and pressure, gas and air properties), and structural behavior (material properties).

Thermal fatigue life in nozzles is directly related to stresses and strains due to thermal gradients generated by combustion gas flow as well as air circulating in the internal cooling system. Tensile stresses induced by low temperatures are the most critical and damaging concerning fatigue failures.

Despite great advances in the metallurgical area to improve efficiency by increasing temperatures, superalloy fatigue properties are affected by these high limiting temperatures turbine operation. Thermo-mechanical loads in hot components should be analyzed, including transient events from the numerical analysis point of view, since measurements in real time are almost impossible in most situations.

Most current mathematical models for fatigue analysis used by designers are merely adaptations to the classical Manson-Coffin equation and variations of the strain partitioning method [1].

The principal factor that makes investigation of fatigue properties difficult during transients is that experimental measurements are practically impossible in high temperature zones.

Three basic type of fatigue can be distinguished: High Cycle Fatigue (HCF), Low Cycle Fatigue (LCF) and Thermo-mechanical Fatigue (TMF). Commonly HCF is associated with low level stresses and highly frequent load fluctuations, while LCF is mainly affected by high amplitudes of stresses and strains of low frequency. TMF simultaneously describes thermal and mechanical strains due to temperatures gradients in time and space and also mechanical loads.

In the present paper, a first stage gas turbine nozzle (MS7001E) is studied in order to obtain thermal fatigue life estimations (LCF). To establish a comparison of several fatigue models, the fatigue life models of Manson-Coffin-Basquin, Morrow and Smith-Watson-Topper were compared assessing nozzle life in different critical zones.

2 NOMENCLATURE

b	Fatigue Strength Exponent
c	Fatigue Ductility Exponent
E	Modulus of Elasticity
$2N_f$	Number of Reversals to Failure
N_f	Number of Cycles to Failure
n´	Cyclic Strain Hardening Exponent
n_1 $n_{2,..}$	Number of Fatigue Cycles
T	Temperature
$\sigma_f´$	Fatigue Strength Coefficient
σ_{max}	Maximum Stress in One Cycle
σ_o	Local Mean Stress
ε_{ae}	Elastic Strain Amplitude
$\varepsilon_f´$	Fatigue Ductility Coefficient
ε_{ap}	Plastic Strain Amplitude
ε_t	Total Strain Amplitude

3 LOAD HISTORIES: STRESSES AND STRAINS DURING TURBINE STARTUP-SHUTDOWN CYCLE

At the beginning of turbine startup, nozzle inner zone temperature is less than at the external surface. This temperature is higher mainly at the leading edge of the nozzle vane, where the main gas flow is attacking. During this process, hot zones tend to expand finding restrictions in cooler zones that cause compression. In other words, during startup, compressive stresses are generated in the hottest side (gas flow interface) and tensile stresses in the cooled section internal surface. On the other hand, during shutdown, a reverse process takes place. Internal temperature is lower at the beginning and becomes higher later with respect to external temperatures. Therefore external surfaces and cooling channels have tensile stresses which can be critical if the process is very fast.

General strain histories at the nozzle vane leading edge during a normal startup-shutdown process are shown in Figure 1 [2].

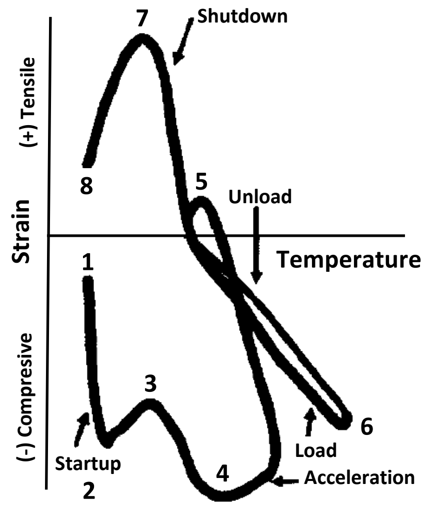

Figure 1 - Strain variation vs. temperature at the vane leading edge during startup-shutdown cycle [2].

Corresponding nozzle stresses and strain histories during a normal startup-shutdown process were determined using a finite element program [1] and the nodal results were used for processing according to the nozzle time strain history shown in Figure 2.

Load history was built considering eight points (Fig 1 and Fig. 2). Points 1 and 3 correspond to unit startup, points 3 and 4 include rotor acceleration, points 5 and 6 represent load increase, point 6 determines turbine full load-steady state and finally points 7 and 8 indicate shutdown under normal conditions.

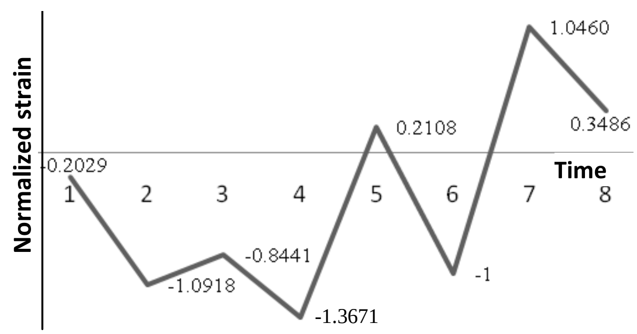

Figure 2 - Strain variation vs. time at the nozzle vane leading edge during startup-shutdown cycle

All values of strains shown in Figure 2 are normalized in proportion to strain at the nozzle leading edge during turbine steady state-full load. It means that the “-1” strain value of point 6 corresponds to strain calculated value at full load (Fig. 1).

4 MATERIAL FATIGUE PROPERTIES

Manson and Coffin proposed an expression to estimate component fatigue life without notches based on uniaxial tension properties. The cycles to cracking (N_f) depend on applied strain amplitude and material properties. On the other hand, Basquin basically applied the same concept but to elastic strain and stress. The well known Manson-Coffin-Basquin model presented in Eqn. 1 [3], estimates cycles to cracking from total strain amplitude neglecting mean stress effects. This model is widely used when strains are elastic plus inelastic when the mean stress is very low or does not exist.

$$\varepsilon_a = \varepsilon a_{ae} + \varepsilon_{ap} = \frac{\sigma_f'}{E}(2N_f)^b + \varepsilon_f'(2N_f)^c \qquad (1)$$

Cycles of similar magnitude but different mean stress cause a different amount of fatigue damage especially in the high cycle fatigue zone, as can be seen in Figure 3. This effect is considered in the Morrow model according to Eqn. 2 [4].

$$\varepsilon_a = \frac{(\sigma_f' - \sigma_o)}{E}\ (2N_f)^b + \varepsilon_f'(2N_f)^c \qquad (2)$$

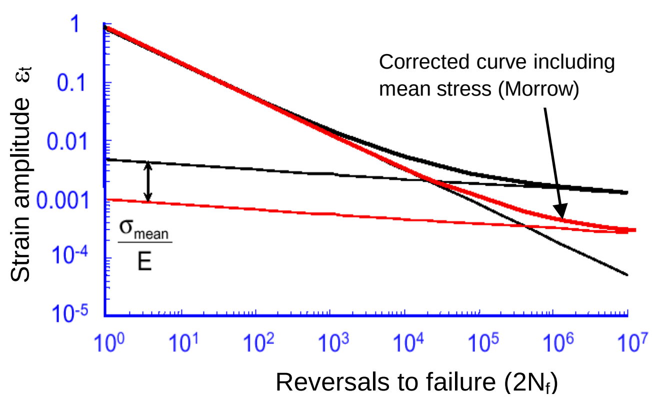

Figure 3 - Mean stress correction (Morrow equation). Notice the main influence in the high cycle zone

Alternatively there can be a combination of damage and stress-strain parameters as proposed by Smith, Watson and Topper (SWT) [5] in Eqn. 3.

$$\sigma_{\max}\ \varepsilon_a = \varepsilon_f'\ \sigma_f'(2N_f)^{b+c} + \frac{\sigma_f'^{\,2}}{E}(2N_f)^{2b} \qquad (3)$$

In this case, the local mean stress effect is taken into account through the maximum stress in the cyclic hysteresis loop. All the above equations can be solved iteratively by numerical methods to obtain the number of cycles to failure N_f.

The required cyclic material properties help define stress-strain and total strain curves. These properties are normally obtained experimentally under controlled deformations and polished materials.

The nozzle is made of cobalt base superalloy FSX-414, and cyclic parameters for this material were obtained from research done by [6, 7 and 8]. Using these experimental data and MathCAD software, Manson's parameters of Eqn. (1) were fitted and are presented in Table 1.

Fatigue properties values shown in Table 1 correspond to several temperatures points from isothermal experiments: 649, 700, 760, 850 and 900°C. By curve fitting regression analysis, the Manson parameters shown in Table 2 were obtained, which allows nozzle fatigue analysis within the wide range of temperatures experienced during the operation cycles.

Table 1 – Manson parameters as stated in Equation 1, cyclic and mechanical properties of FSX-414 at different temperatures [6, 7 and 8].

Parameter	649°C	700°C	760°C	850°C	900°C
σ_f' (MPa)	461.36	415.24	363.869	316.48	280.85
ε_f' (-)	0.382193	0.352213	0.325261	0.29097	0.26328
b	-0.08975	-0.10444	-0.118848	-0.12962	-0.14325
c	-0.52288	-0.56742	-0.59246	-0.62278	-0.64083

With the obtained polynomials (Table 2), it is possible to interpolate and extrapolate to get fatigue properties at different temperatures but not too far from the range shown in Table 1. As can be seen, fatigue property variation is practically linear with temperature.

Table 2 - Manson parameters, cyclic and mechanical properties as a function of temperature (in °C)

Parameter	Polynomial equation
σ_f' (MPa)	$1185.7 - T$
ε_f' (-)	$0.1617 + 0.0001T$
b	$-0.036 - 0.0001T$
c	$-0.2050 - 0.0005T$

Figure 4 shows the fatigue curves of material FSX-414 corresponding to 500, 600, 700, 800 and 900 °C obtained by curve fitting using the Manson parameters shown in Table 2. These data were used to calculate nozzle thermal stresses and thermal fatigue, which are analyzed in the following sections.

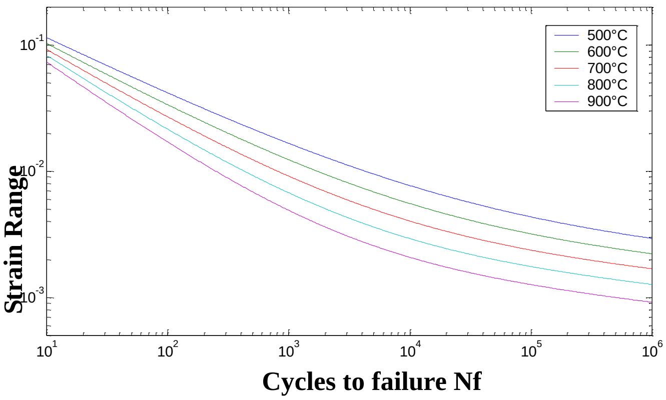

Figure 4 - Fatigue curves for FSX-414 at different temperatures obtained by curve fitting 500, 600, 700, 800 and 900°C (Eqn. 1)

5. COUNTING OF FATIGUE CYCLES USING RAINFLOW METHOD

Most real-life structures experience complex load histories that rarely have constant amplitude. In order to analyze real-life structures under these complex loads, the load history has to be reduced. The complex loads are divided into blocks of constant amplitude loads using a process called 'cycle counting'. The damage accumulated due to these constant amplitude blocks can be calculated individually and summed using Palmgren-Miner-Rule to calculate the total accumulated damage of the structure.

The rainflow-counting is used in the analysis of fatigue data in order to reduce a spectrum of varying stress (long complex strain history) into a set of simple stress reversals and count hysteresis loops. The rainfow counting method is widely used to decompose an arbitrary sequence of loads or deformations into cycles and to count those cycles. The single cycle, respectively the corresponding hysteresis loop in the stress-strain plane certainly constitutes a basic event for damage assessment. In combination with the Palmgren-Miner-Rule, we thus obtain for every sequence of loads a real number which estimates the damage inflicted upon the workpiece by this loading sequence. Its importance is that it allows the application of Miner's rule in order to assess the fatigue life of a structure subject to complex loading. The algorithm was developed by Tatsuo Endo and M. Matsuishi in 1968 [9]. Downing and Socie created one of the more widely referenced and utilized rainflow cycle-counting algorithms in 1982 [10] which was included as one of many cycle-counting algorithms in ASTM E 1049-85 [11]. Counting is carried out on the basis of the stress-strain behavior of the material. Igor Rychlik gave a mathematical definition for the rainflow counting method [12] thus enabling closed-form computations from the statistical properties of the load signal.

Cycle counting is used to summarize (often lengthy) irregular load-versus-time histories by providing the number of times cycles of various sizes occur. The definition of a cycle varies with the method of cycle counting. ASTM E1049 cover the procedures used to obtain cycle counts by various methods, including level-crossing counting, peak counting, simple-range counting, range-pair counting, and rainflow counting. Cycle counts can be made for time histories of force, stress, strain, torque, acceleration, deflection, or other loading parameters of interest.

The single cycle and the corresponding hysteresis loop in the stress-strain plane which constitutes a basic event for damage assessment is related to Baushinger Effect.

When materials are loaded uniaxially in one direction (e.g. in tension) into the plastic regime, unloaded to zero stress level, then reloaded in reverse direction (e.g. in compression), they may yield during the reloading, at a stress level lower than if the reloading were carried out in the original direction [13]. This effect is observed even the straining is in the same direction as the previous straining. A hysteresis loop can be observed to reach the same value of straining as the previous one. This direction-dependent, asymmetrical yield behavior is known as the Bauschinger effect, after Johann Bauschinger [14] who first reported this phenomenon in 1886. Further work revealed the effect to be more complex and several parameters were developed to assess this affect [15-20]. There are two principal Bauschinger effect theories; back stress and Orowan theory [15, 19]. The basic mechanism for the Bauschinger effect is related to the dislocation structure in the cold worked metal. As deformation occurs, the dislocations will accumulate at barriers and produce dislocation pile-ups and tangles. During forward plastic deformation moving dislocations interact with different obstacles (other dislocations, grain boundaries and precipitates) preventing their further propagation. The pile-up of dislocations at grain boundaries and Orowan loops around strong precipitates generates a back stresses around the contact point resisting further progress of similarly signed dislocations. During the reverse deformation this back stress repels the dislocations from the obstacles in the opposite direction, namely in the direction of reverse strain. Thus the stress field helps to move the dislocation in the direction of reverse strain and the reverse yield stress drops by the level of the back stress. The Bauschinger effect is important as it appears to be the basis for low hardening rates and low saturation stresses (and failure stresses) in cyclic deformation.

The Rainflow method is widely used to account for fatigue cycles and fatigue life assessment because it follows the hysteresis cycle of stress-strain curve [21]. In Figure 5 the building of hysteresis cycles from strain history is shown (Fig. 2). The central idea of Rainflow method is to consider small cycles as interruptions of other larger cycles, extracting, in this manner, different individual cycles into the block of data of load history. The application of this method to the turbine startup-shutdown cycle (Fig. 2) is shown in Figure 6, where 3 small cycles (sub cycles) extracted from the principal complete cycle of turbine startup-shutdown can be appreciated. In Figure 5 and Figure 6 the point A corresponds to turbine startup, point B to acceleration, point C to loading, point D to unloading and point F to shutdown.

Fatigue analysis of the nozzle was carried out using individual cycles within the turbine normal startup-shutdown cycle shown in Figure 6. The strains at points A to F of fatigue cycles were obtained for each node of the numerical model of the nozzle from structural analysis using FEM code [1] and were applied to determine fatigue damage.

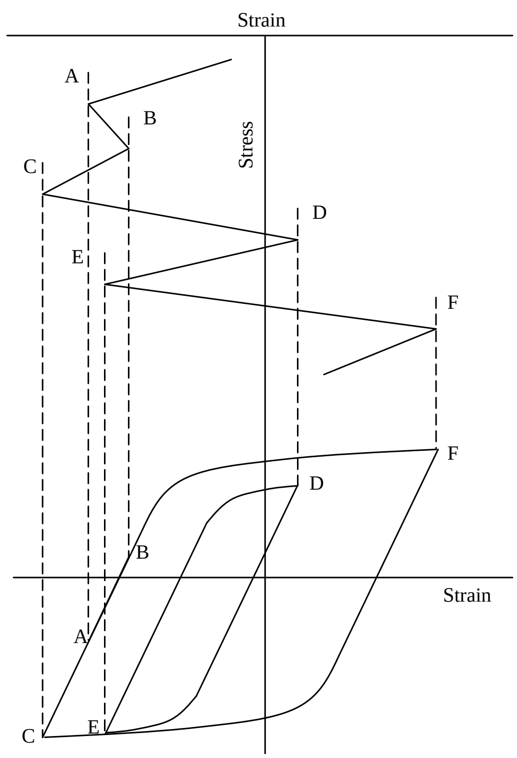

Figure 5 - Illustration of Rainflow procedure.

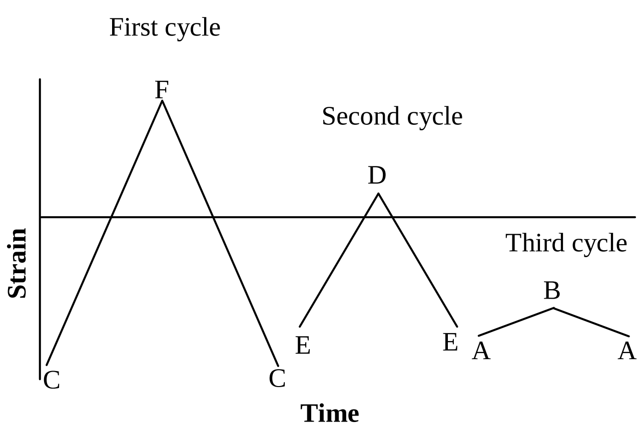

Figure 6 - Extraction of the three small cycles from a single turbine startup-shutdown cycle

The strain magnitudes of points C and F (First cycle), points E and D (Second cycle), points A and B (Third cycle) were introduced to the Manson-Coffin-Basquin equations (Eqn. 1), Morrow (Eqn. 2) and Smith-Watson-Topper (Eqn. 3) to get the number of cycles (N_f) to failure for each fatigue cycle and fatigue model.

Total nozzle fatigue life was determined according to the Miner law from Eqn. (4) for each fatigue model.

$$\frac{n_1}{N_{f1}}+\frac{n_2}{N_{f2}}+\frac{n_3}{N_{f3}}+\cdots=1 \tag{4}$$

This process was repeated for each nodal values of nozzle deformation to get useful life for the whole nozzle body. Nozzle fatigue life was analyzed applying specialized nCode software [22] using its module: Critical Location Fatigue (CLF). First, it was necessary to determine material fatigue properties related to temperature at each nozzle zone (node) and next to build related load history considering calculated strains. Figure 7 shows strain history for one nozzle critical zone (Zone 4, Figure 8; vane to internal shroud transition on the suction side).

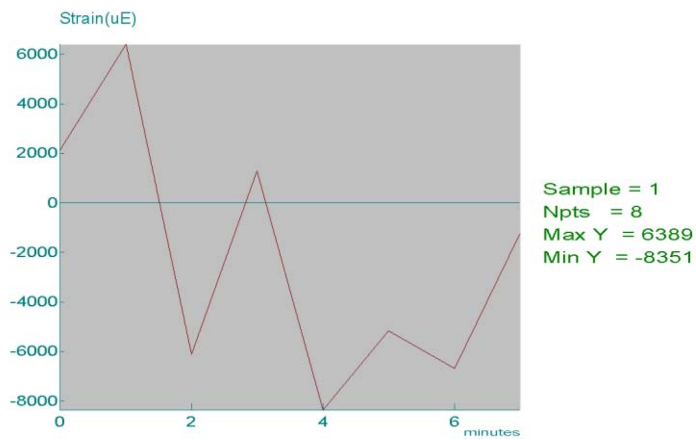

Figure 7 - Load history of Zone 4 (Fig. 8) during a turbine startup-shutdown cycle obtained from nCode software.

Temperatures in each node of the FEA model were calculated for steady state at full load of turbine and for the transient state (startup-shutdown cycle) previously by means of CFD analysis [23]. The external surface temperature distribution was validated/compared to a similar vane [24]. This vane temperature distribution was very similar qualitatively to the one obtained in this analysis. Then these values were considered in each cycle point to point by modifying mechanical and fatigue properties as a function of temperature. In this manner, stresses and strains were calculated at their specific temperature. All these stress and strain histories were then used in the fatigue life assessment.

It is important not to forget the statistical nature of fatigue due to the variability in fatigue test results and material properties scatter. Moreover, there are also certain inaccuracies of the thermal boundary conditions from the CFD analysis. So, the fatigue life results are considered good in general but they can be later compared with those corresponding to other boundary conditions or even other material properties considering aging of material.

6 - NOZZLE FATIGUE LIFE ASSESSMENT

Results for the whole nozzle body fatigue life (cycles to failure) during startup-shutdown cycles applying the Morrow prediction model are shown in Figure 8. The zones of shorter life are located in cooling channels on the pressure side (Zone 3) and at the vane to inner shroud transition on the convex side (Zone 4).

There is some similarity of nozzle fatigue life results comparing the Morrow model to the Manson-Coffin-Basquin model, particularly in the high strain zones as shown in Table 3. In general, the Morrow model provides slightly higher nozzle fatigue life than the Manson-Coffin-Basquin model in high strain zones (0.003 to 0.006 mm/mm) and clearly higher in lower strain zones (0.000 to 0.002 mm/mm). In the case of the Smith-Watson-Topper model, nozzle life is slightly lower in high strain zones and clearly lower in lower strain zones compared to the Manson-Coffin-Basquin model.

Summarizing the fatigue prediction results of all analyzed models, it can be concluded that they show good concordance in zones of high strain - high stress (low cycles) and some divergence in zones of low strain-low stress (high cycles). These variations may be attributed to different ways of considering mean stress effects at each model (see Eqn1, Eqn.2, Eqn.3 and Fig. 3).

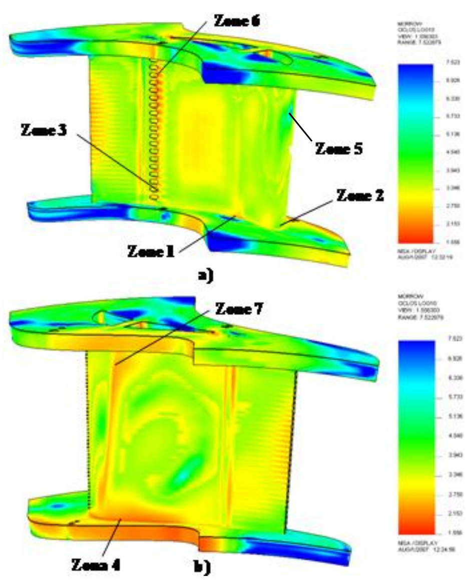

Figure 8 - Nozzle life (cycles to failure) during startup-shutdown cycles using the Morrow prediction model. a) Pressure side, b). Suction side.

It is important to notice that because the finite element method was used for stress/strains calculations, for estimation of fatigue lives, geometry effects like stress concentrations are already taken into account. In this manner, life results in some critical zones of the nozzle like fillets and film cooling holes consider these high stresses.

Table 3 - Nozzle fatigue life estimation during transitions

Zone	Node No.	Temp. (°C)	Total strain (mm/mm)	Stress Von Mises (MPa)	Life (MCB) (cycles)	Life (M) (cycles)	Life (SWT) (cycles)
1	38737	779	0.003073	402.98	805	837	778
2	92588	792	0.002223	379.52	1637	1723	1476
3	14853	777	0.003967	414.34	454	467	442
4	162580	741	0.006109	319.35	223	227	215
5	94192	1062	0.000816	121.55	12017	14197	7559
6	22098	767	0.001868	374.45	3349	3532	2853
7	149553	776	0.002751	395.90	1078	1128	1029

MBC: Manson-Coffin-Basquin, M: Morrow, SWT: Smith-Watson-Topper

Additionally, the hysteresis cycles used for fatigue analysis are shown in Figure 9, where three individual cycles were generated by the CLF module on the basis of nozzle load history and previously defined nozzle material properties.

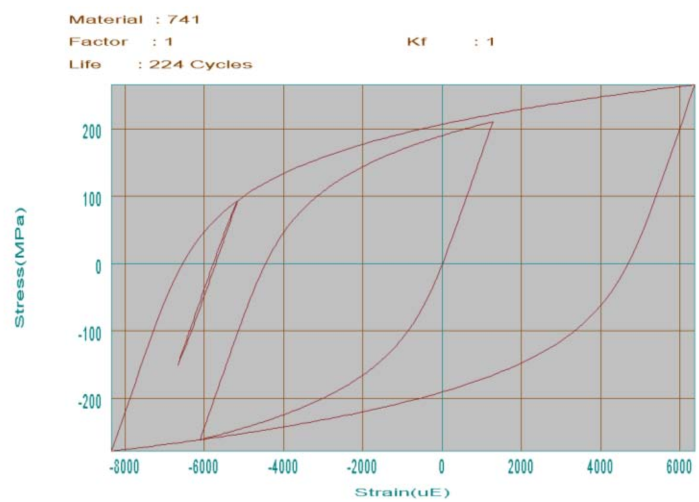

Figure 9 - Three hysteresis cycles during a startup-shutdown cycle corresponding to Zone 4 of the nozzle (see Fig. 8)

Figure 10 shows thermal fatigue cracks in the analyzed nozzle retired from service. The nozzle operated 54000 hours and had accumulated at least 136 startup-shutdown cycles. Cracks were detected at the internal cooling holes and vane airfoil near the nozzle internal and external shroud, which are zones of high strains and also high gradients of temperatures. The cracks initiated around the cooling holes on the airfoil and at the trailing edge and then propagated into the solid body following through the grains trajectory [25]. Crack size reached between 15 mm to 80 mm depending on location. It was evaluated that crack initiation and propagation were driven by a fatigue mechanism with a great influence of creep damage. High stresses at elevated temperatures contributed to crack propagation as long as fatigue mechanism [25]. This interaction between creep and fatigue was not studied here. Comparing crack distribution on the real nozzle retired from service (Fig. 10) to the nozzle life distribution obtained by numerical prediction (Fig. 8), good concordance was found. It should be noticed that it was not only the fatigue mechanism that produced the final failure, but also the creep mechanism had an important contribution to it. It would have been good to take it into account by considering hold times curves of fatigue but they were not available, instead only high temperatures fatigue curves were used. Creep damage was evident when metallurgical inspection was made.

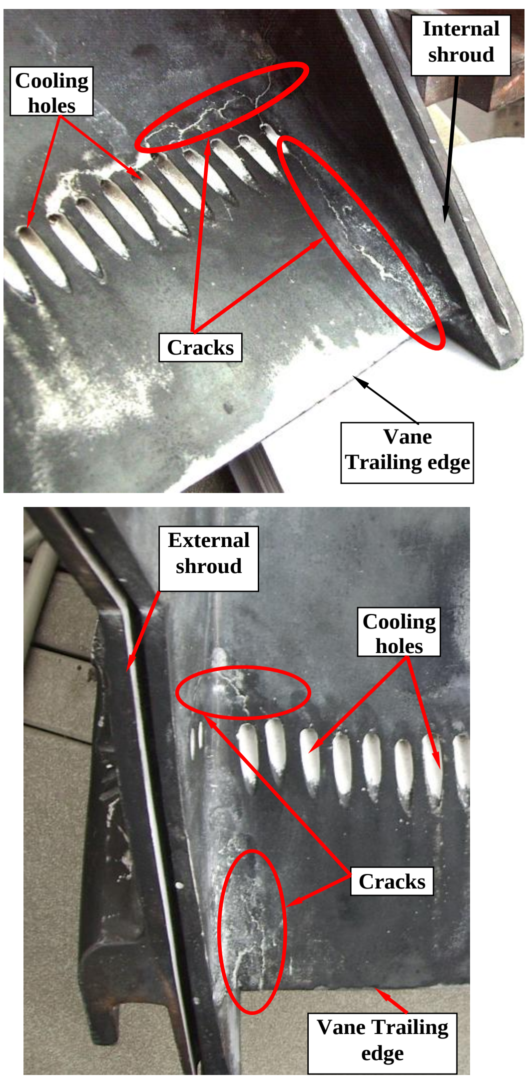

Figure 10 - Thermal fatigue cracks on the nozzle vane

7 CONCLUSIONS

Fatigue analysis of a 70 MW gas turbine first stage nozzle was carried out using Manson-Coffin-Basquin, Morrow, y Smith-Watson-Topper models.

The zones of shorter nozzle life are located in cooling channels and at the vane to shrouds transitions. Local stress concentrations were considered implicitly through the finite element model.

There is some similarity in nozzle fatigue life results comparing Morrow and Smith-Watson-Topper models to the Manson-Coffin-Basquin model, particularly in the high strain zones.

In general, the Morrow model provides slightly higher nozzle fatigue life than the Manson-Coffin-Basquin model in high strain zones and clearly higher in lower strain zones. In the case of the Smith-Watson-Topper model, nozzle life is slightly lower in high strain zones and clearly lower in lower strain zones compared to the Manson-Coffin-Basquin model.

Comparing the fatigue prediction results of all analyzed models, it can be concluded that they show good concordance in high strain zones (high strains - high stress) and shows some divergence in low strains-low stress zones.

The method presented is intended to be used in critical zones only or several ones, one at a time. The most adequate method for counting cycles seems to be the Rainflow cycle counting method, which is widely used. This analysis requires knowledge of stresses and strains in a critical zone of the nozzle. However, assessment of these values requires great effort by means of finite elements and CFD. Once stresses and strains were obtained, it was possible to accomplish fatigue analysis using this methodology.

Comparing crack distribution on the real nozzle retired from service to nozzle life distribution obtained by numerical predictions of all analyzed models, good concordance was found. It should be noticed that a complete analysis would include creep and fatigue interaction.

8 REFERENCES

[1] Pérez-Hernández E.B, 2007, “Life Consumption Analysis due to Thermal Fatigue in Gas Turbine Nozzles during Continuous and Transient Loads”, National Research and Technological Center, MSc. Thesis (in Spanish), Cuernavaca, Mexico.

[2] Brandt D.E. and Wesorick R.R., 1994, “GE Gas Turbine Design Philosophy”, GER3434D, New York, pp.18.

[3] García-Illescas R. and Mazur Z., 2006, “Comparisons of Some Fatigue Models and Their Application to Gas Turbines Hot Components”, 9th International Fatigue Congress, Atlanta, Georgia, pp. 1-10.

[4] Morrow JD., 1964, “Cyclic Plastic Strain Energy and Fatigue of Metals”, Internal Friction, Damping, and Cyclic Plasticity – ASTM STP 378, American Society for Testing and Materials, Philadelphia, pp. 45-87.

[5] Smith K.N., Watson P. and Topper T.H., 1970, “A Stress-Strain Function for the Fatigue of Metals”, ASTM Journal of Materials **5** (4), pp. 767– 778.
[6] Flowers, T. L., Anderson, A. W., and Brunso, J., 1979, “Improvement of Nozzle Life in Gas Turbines”, American Society of Mechanical Engineers, Vol. 79-GT-50, pp. 12-18.
[7] González J.L., 1999, “Metalurgia Mecánica”, Noriega Limusa, México, D.F., pp. 210-211.
[8] Viswanathan R., 1995, “Damage Mechanisms And Life Assessment Of High–Temperature Components”, ASME International, pp. 420-421.
[9] Matsuishi, M. & Endo, T. (1968) Fatigue of Metals Subjected to Varying Stress, Japan Soc. Mech. Engineering.
[10] Downing, S. D., Socie, D. F. (1982). Simple Rainflow Counting Algorithms. International Journal of Fatigue, Volume 4, Issue 1, January, 31-40.
[11] ASTM E 1049-85. (Reapproved 2005). Standard Practices for Cycle Counting in Fatigue Analysis. ASTM International.
[12] Rychlik, I. (1987) A New Definition of the Rainflow Cycle Counting Method, Int. J. Fatigue 9:2, 119-121.
[13] Dowling, Norman.E., Mechanical Behavior of Materials, Prentice Hall, 1993, p.339-396.
[14] Bauschinger S. J., Mechanisch-Technischen Laboratorium, Materials Forum, 1886.
[15] Abel A. and Muir H., The Bauschinger Effect and Discontinuous Yielding, Philosophical Magazine, Vol. 26, 1972, p. 489 – 504.
[16] Bate P.S. and Wilson D.V., Analysis of the Bauschinger Effect. Acta Metallurgica, Vol. 34, № 6, 1986, p. 1097 - 1105.
[17] Abel, A., Historical Perspectives and Some of the Main Features of the Bauschinger effect, Materials Forum, Vol. 10, № 1, 1987, p. 11 – 26.
[18] Embury J.D., Structural Aspects of the Bauschinger Effect, Materials Forum, Vol. 10, № 1, 1987, p. 27 – 32.
[19] Brown L.M., Orowan’s Explanation of the Bauschinger effect, Scripta Metallurgica, Vol. 11, 1977, p. 127 – 131.
[20] Thakur, A., Vescchio, K.S. and Nasser, S.N. “Bauschinger Effect in Haynes 230 Alloy: Influence of Strain Rate and Temperature.” Met. Trans. A., 27a (1996), 1739-1747.
{21] Strang A, 1983, “High Temperature Properties of Coated Superalloys”, GEC Turbine Generators Limited, Whetstone, Leicester, U.K., pp. 595-611.
[22] nCode “On – Line Manual of CLF”, Version 5.3, 2001.
[23] Mazur Z., Hernandez-Rossette A., Garcia-Illescas R. and Luna-Ramirez A., Analysis of Conujgate Heat Transfer of a Gas Turbine First Stage Nozzle, ASME Turbo Expo, June 6-9, 2005, Tahoe, Nevada, USA.
[24] EPRI report AP-4751, Project 1319-5, Advanced Cooled-Engine Shell/Sapare Turbine Vanes and Blades, August 1986.
[25] Mazur Z., Hernandez-Rossette A., Garcia-Illescas R. and Luna-Ramirez A., 2008, “Failure Analysis of a Gas Turbine Nozzle”, Engineering Failure Analysis **15**, pp. 913–921.